Available online at www.sciencedirect.com

ScienceDirect

Energy Procedia 63 (2014) 2510 – 2529

Energy Procedia

GHGT-12

CO2PipeHaz: quantitative hazard assessment for next generation CO_2 pipelines

Robert M. Woolley[a,*], Michael Fairweather[a], Christopher J. Wareing[a], Samuel A.E.G. Falle[b], Haroun Mahgerefteh[c], Sergey Martynov[c], Solomon Brown[c], Vagesh D. Narasimhamurthy[d], Idar E. Storvik[d], Lene Sælen[d], Trygve Skjold[d], Ioannis G. Economou[e], Dimitrios M. Tsangaris[e], Georgios C. Boulougouris[e], Nikolaos Diamantonis[e], Laurence Cusco[f], Mike Wardman[f], Simon E. Gant[f], Jill Wilday[f], Yong Chun Zhang[g], Shaoyun Chen[g], Christophe Proust[h], Jerome Hebrard[h] and Didier Jamois[h]

[a]*School of Chemical and Process Engineering, University of Leeds, Leeds LS2 9JT, UK,* [b]*School of Mathematics, University of Leeds, Leeds LS2 9JT, UK,* [c]*Department of Chemical Engineering, University College London, London WC1E 7JE, UK,* [d]*GexCon AS, P.O. Box 6015, Bergen Bedriftssenter, Bergen NO-5892, Norway,* [e] *National Center for Scientific Research "Demokritos", Aghia Paraskevi, Attikis GR–153 10, Greece,* [f]*Health & Safety Laboratory, Harpur Hill, Buxton SK17 9JN, UK,* [g]*School of Chemical Engineering, Dalian University of Technology, Dalian, People's Republic of China,* [h]*INERIS, Parc Technologique ALATA, Verneuil-en-Halatte BP 2, 60550, France*

Abstract

Without a clear understanding of the hazards associated with the failure of CO_2 pipelines, carbon capture and storage (CCS) cannot be considered as a viable proposition for tackling the effects of global warming. Given that CO_2 is an asphyxiant at high concentrations, the development of reliable validated pipeline outflow and dispersion models are central to addressing this challenge. This information is pivotal to quantifying all the hazard consequences associated with the failure of CO_2 transportation pipelines, which forms the basis for emergency response planning and determining minimum safe distances to populated areas. This paper presents an overview of the main findings of the recently completed CO2PipeHaz project [1] which focussed on the hazard assessment of CO_2 pipelines to be employed as an integral part of CCS. Funded by the European Commission FP7 Energy programme, the project's main objective was to address this fundamentally important issue.

Peer-review under responsibility of the Organizing Committee of GHGT-12

Keywords: CCS; CO_2; multi-phase flow; atmospheric dispersion; mathematical modelling; pipeline depressurisation; experimental measurement

* Corresponding author. Tel.: +44-113-343-2351; fax: +44-113-343-2384.
E-mail address: r.m.woolley@leeds.ac.uk

Peer-review under responsibility of the Organizing Committee of GHGT-12
doi:10.1016/j.egypro.2014.11.274

1. Introduction

Whilst the physics of high-pressure releases of substances such as natural gas and propane is relatively well understood [2, 3], CO_2 possesses some unusual physical properties which make its release behaviour more challenging to predict. For example, CO_2's triple-point pressure and temperature are 5.18 bar and 216.55 K respectively, and at atmospheric pressure CO_2 exists in either a solid or gaseous state, with a sublimation temperature of 194.25 K. This means there will be complex dynamics, involving multiple phase transitions, observed when CO_2 decompresses from an initial dense-phase state in the pipeline (i.e. as a supercritical or liquid fluid) into a solid and gaseous state at atmospheric pressure. The work undertaken in the EC FP7 CO2PipeHaz project [1] has been pivotal to improving the understanding of this complex behaviour in order to provide more accurate predictions of the consequences associated with CO_2 pipeline releases. Subsequently, this forms the basis for emergency response planning and determining minimum safe distances to populated areas for operational pipelines.

The development of the state-of-the-art multi-phase heterogeneous discharge [4] and near- and far-field dispersion models [5, 6] for predicting the correct fluid phase during the discharge and dispersion processes have received special consideration given the very different hazard profiles of CO_2 in the gas and solid states. Model validations were based on small-scale controlled laboratory conditions [7], medium-scale experimental investigations [8], and also large scale field tests performed using a specially designed, constructed, and fully instrumented, 250 m long section of 0.23 m internal-diameter pipeline in China. The large-scale experiments involved the full-bore rupture and puncture of the pipeline containing dense phase CO_2 charged to a maximum pressure of 80 bar, and the heterogeneous flow patterns in the ruptured pipe and the near-field dispersion region were investigated in both the small- and medium-scale experiments. These experiments were modelled in order to obtain a complete understanding of the discharge phenomena and gas-plume behaviour following a large-scale CO_2 release, thus providing the basis for calculating the minimum safe distances.

With respect to the pipeline outflow modelling [4], a homogeneous relaxation model (HRM) accounts for the delay in vaporisation during the decompression process using an empirical relaxation equation for the mass fraction of vapour phase, whilst assuming that the constituent phases are in mechanical equilibrium, i.e. that they move at the same velocity. In this approach, conservation equations for the mass, momentum, energy and vapour quality are solved, which requires an equation of state (EoS) to close the model. Accurate and efficient prediction of the thermodynamic properties of CO_2 through the implementation of such an EoS is key to successful modelling of accidental releases from pressurised transportation pipelines. In addition to the development of a unique composite equation of state describing the behaviour of the three phases of pure CO_2 [9], work was undertaken to develop advanced thermodynamic methods based upon SAFT (statistical associating fluid theory) modelling strategies [7].

For the near-field modelling, the calculations employed an adaptive finite-volume grid algorithm which used a three-dimensional rectangular mesh to solve the density-weighted averaged Navier-Stokes equations. The model to describe the fluid flow-field employed in this study was cast in an axisymmetric geometry for the validatory calculations of jet releases. A full three-dimensional scheme was applied to crater release calculations although the use of symmetry boundaries aided a reduction in computational expense. A full description of the equations solved is reported elsewhere [5].

Far-field modelling of the dispersion of two-phase (gaseous and particulate) CO_2 was undertaken using two different commercial computational fluid dynamic (CFD) codes: FLACS [10]; and ANSYS-CFX [11]. In both cases, the continuous gas-phase flow was simulated in the Eulerian reference frame, while a Lagrangian formulation was used for the dispersed particulate phase. The source-term boundary condition for the far-field dispersion modelling was constructed using predictions from the near-field dispersion model, which consisted of integrated planar profiles of density, pressure, velocity, temperature, CO_2 solid and gas concentration, turbulence kinetic energy and its dissipation rate. In each case, a realistic terrain was used to simulate the impact of typical geographical features on the flow dynamics.

This work has demonstrated that it is feasible to simulate industrially-relevant flows associated with CCS operations, and the understanding gained in the execution of this project has been used for evaluating the adequacy of control measures for CO_2 pipelines, with best practice guidelines being developed. Further, a risk assessment methodology has been developed and decision support tools validated. The usefulness of the technologies developed were demonstrated in application to a test-case pipeline in a realistic-terrain scenario.

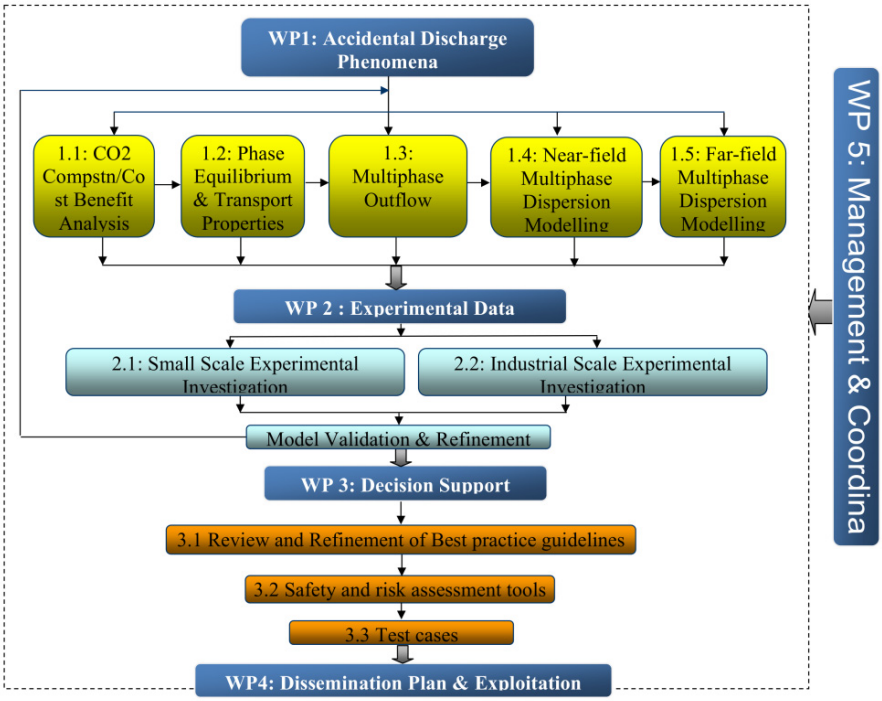

Fig. 1. Pert diagram representation of the CO2PipeHaz project structure.

2. Project work packages

The CO2PipeHaz project structure can be schematically represented as Figure 1, and in what follows is a description of each of the technical WP contributions and their interactions. Also discussed are their significant outputs with respect to technological developments and demonstrations.

2.1. WP1 - Accidental discharge phenomena

2.1.1. WP1.1 - CO_2 Composition and cost benefit analysis

The work undertaken in this package underpinned other project activities by examining likely CO_2 composition delivered to pipelines. Likely ranges for the composition of captured CO_2, and factors affecting those ranges, were identified for a number of CO_2 capture technology options including post-combustion, pre-combustion and oxyfuel [12]. Assessments of the requirements for CO_2 purification, through minor component and impurity removal from CO_2 mixtures, in order to protect pipelines during transportation and the environment following accidental release were carried out. In particular, heavy metals such as mercury and arsenic are highly hazardous, and must be removed completely. Acidic gases such as SO_2, HCl, NO_x and H_2S in the presence of water would lead to corrosion to the pipe wall. On the other hand, small gaseous molecules such as H_2, N_2 and O_2 would penetrate and damage the pipeline material. Recommendations were made regarding acceptable CO_2 compositions and required purification methods. The costs for achieving higher CO_2 purity were assessed on the basis of estimates for the reduced performance such as operating costs and capture level, and also increased capital costs [13]. Further to this, a suggested composition range for CO_2 streams during pipeline transport was reported [14], based upon the cost impact of the presence of such impurities, and is reproduced as Table 1.

Table 1. Recommended impure CO_2 composition range from CO2PipeHaz Project.

Species	Part of total composition
CO_2	>95.5 %/vol
N_2, O_2, H_2, Ar, CH_4	4 %/vol maximum. No individual >2 %/vol
H_2O	≤50 p.p.m.
SO_x	≤100 p.p.m.
NO_x	≤100 p.p.m.
H_2S	≤200 p.p.m.
CO	≤2000 p.p.m.
C_2H_6 - C_4H_{10}	≤0.5 %/vol

2.1.2. WP1.2 - Phase equilibrium and thermodynamic and transport properties

The efficacy of the outflow and dispersion models developed in WP1.3, WP1.4 and WP1.5, critically depends upon the use of accurate and computationally efficient equations of state for providing the pertinent thermodynamic and phase equilibrium properties. In this work package, new models were developed in order to accurately, efficiently and vigorously predict the properties of pure CO_2 and its mixtures with components of interest to CCS transport. All thermodynamic models developed in this work were included in the Physical Properties Library (PPL). The PPL is an evolving software package linkable by third parties which encapsulates theoretical and engineering models capable of predicting the thermophysical properties of CO_2 and its mixtures. Supported properties include volumetric properties (density, compressibility), energy (enthalpy, entropy, heat capacity), free

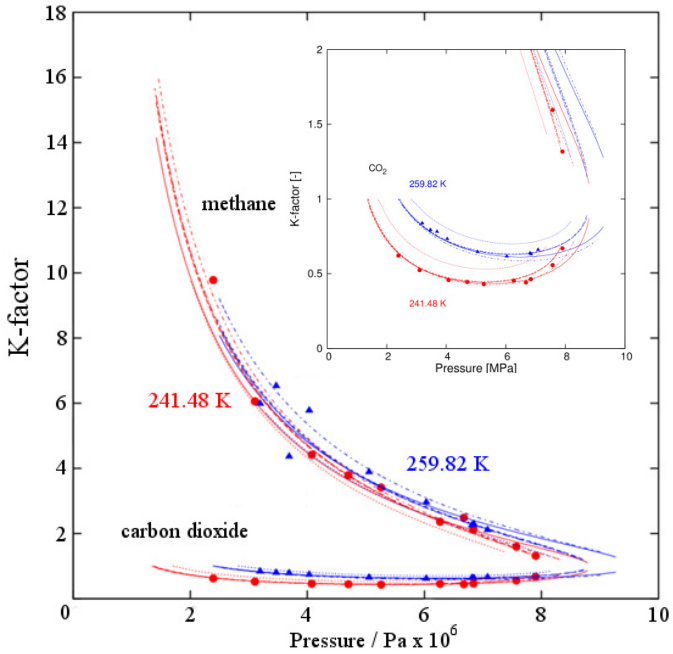

Fig. 2. K-factor (y/x)/pressure diagram for CO_2 – CH_4 mixture. Experimental data (points) and calculations from RK (·····), SRK (—·—·—·—), PR (— — — — —), PR/G (▪ ▪ ▪ ▪ ▪ ▪ ▪), SAFT (– · – · – · –), and PC-SAFT (———). Top: predictions ($k_{ij} = 0$), bottom: correlations ($k_{ij} \neq 0$).

energy and fugacity, in addition to derivative properties (speed of sound, Joule-Thompson coefficient) and transport properties (viscosity, diffusivity, conductivity). The latest version can predict the thermodynamic and transport properties of CO_2 using a variety of EoS including simple cubic EoS (Redlich-Kwong (RK), Soave-Redlich-Kwong (SRK) and Peng-Robinson (PR) [15]), specialized EoS such as GERG [16] and Yokozeki [17], and advanced EoS such as SAFT, PC-SAFT and tPC-PSAFT. The aim of work undertaken was hence the development of a 'platform' capable of predicting physical and thermodynamic properties of pure CO_2 and its mixtures which can be used by all partner models regardless of scope, type and capabilities (one dimensional homogenous models, near-field CFD, far-field CFD, etc). The package is written in C++ and in order to link the PPL to partner computer codes, interfaces in C++ and Fortran have been developed.

SAFT and PC-SAFT (perturbed chain-SAFT) equations of state have been applied within the PPL to predict thermodynamic properties of pure CO_2 and other gases of interest to CO_2 transportation via pipelines. Calculations have been performed over a wide range of temperature and pressure conditions, and both phase equilibrium and single phase thermodynamic properties were considered, including vapour pressure, liquid density, heat capacities and speed of sound. Representative results for the K-factors (ratio of mole fraction in the vapour phase to the mole fraction in the liquid phase) of a CO_2/CH_4 mixture are shown in Figure 2. In addition, new viscosity models for CO_2 have been investigated and incorporated into the equations of state, and predictions are in very good agreement with experiments at low and high pressures. Further information regarding the implementation of SAFT and PC-SAFT can be found in Diamantonis and Economou [18] and Diamantonis, et al. [19]

2.1.3. WP1.3 - Multi-phase heterogeneous discharge model and emergency isolation

The rupture or puncture of a CO_2 pipeline results in an expansion wave that propagates away from the release plane towards its intact end with the speed of sound. This wave imparts a drop in pressure which in turn results in a series of expansion waves which propagate into the disturbed fluid. These waves result in the acceleration of the fluid particles in the opposite direction, and hence outflow. The development of a rigorous outflow model therefore requires the precise tracking of these expansion waves and their propagation as a function of time and distance along the pipeline. This involves detailed consideration of several competing and often interacting factors including heat and mass transfer, unsteady fluid flow and thermodynamics. The fact that the speed of sound is markedly affected by the state of the fluid means that the model must also incorporate an accurate equation of state. Due consideration must also be given to the effects of friction which is both flow and phase dependent. More specifically, in the case of CO_2 pipelines, the widely different densities of gas, liquid and solid during the highly transient flows will very likely lead to phase slip and hence non-equilibrium or heterogeneous flow. As mentioned previously, this will directly impact the physical state of the escaping fluid and hence its hazard profile including its dispersion characteristics and erosion behaviour. In this WP, development of a model for outflow from a CO_2 pipeline following pipeline failure was undertaken, and validated against the small-scale experimental data obtained in WP2.1. The model was then extended to simulate the impact of emergency valve closure on mitigating pipeline failure by limiting outflow.

Firstly, a homogeneous relaxation model for simulating outflow following the rupture of dense phase CO_2 pipelines undergoing a phase change during decompression was constructed. The pertinent CO_2 thermodynamic and phase behaviour data were obtained using a cubic equation of state in the first instance, but given the importance of accurate predictions of the thermodynamic properties, a highly accurate thermodynamic model based on the PC-SAFT equation of state, described in section 2.1.2, was also employed. Non-equilibrium vapourisation was accounted for through the addition of a thermodynamic relaxation equation for the vapour evolution to the conservation equations for the mass, momentum, energy and vapour quality followed by their numerical solution. Further details of this equation set and its solution can be found in Brown and Martynov [4].

The flow model's robustness was first successfully demonstrated by analysing the transient in-pipe fluid flow profiles using hypothetical shock tube tests for both liquid and two-phase CO_2. The data showed the marked reduction in the vapourisation rate, and hence a greater propagation speed of the rarefaction wave with increase in the relaxation time. Given that the former dictates the ductile fracture propagation length, over-estimating the pipe wall thickness may be required in order to arrest fracture which would lead to higher costs.

Table 2. Discharge properties predicted using various equations of state in comparison with experimental observation.

Equation of State	Flow Rate / kg s^{-1}	Density / kg m^{-3}	Pressure Drop from Reservoir / bar	Temperature / K	Liquid Phase Fraction
PR	0.76	1047.11	1.64	253.80	1
SRK	0.66	922.10	1.28	253.97	1
PC-SAFT	0.67	1022.85	1.31	254.21	1
Experiment	0.80 (±0.08)	-	-	265.00	-

The comparison of the model predictions with the data obtained from the full bore rupture experiment performed by INERIS as part of WP2.1, produced reasonable agreement [4]. Within the ranges tested, it was found that delayed phase transition has negligible impact on the pipeline depressurisation rate. A similar level of agreement was obtained when the model was also applied to steady state vessel releases. Similar comparisons of the model predictions were made for the experiments involving punctures, and sample results are presented alongside experimental observations in Table 2. This particular release was a 6 mm puncture with a reservoir pressure of 28.4 bar. In this case, the agreement up to approximately 1 s was reasonable, but following this, the decompression rate predicted and the resultant temperature drop was shown to overestimate that observed experimentally. This behaviour is likely due to the assumption of equal velocities between the liquid and vapour phases. While this assumption is found to be valid for full bore rupture, during pipeline punctures observations have shown that phase stratification occurs, in which case phase slip cannot be ignored.

Output from the release model was ultimately used in a hypothetical pipeline release test-case using realistic terrain, which is reported by Woolley, et al. [20]. This case considered a full-bore guillotine rupture at 84 km from the feed end of a 0.9144 m (36 inch) internal diameter, 217 km pipeline, transporting pure CO_2 at 150 bar and 283 K. Along the pipeline length there were assumed to be two emergency shutdown valves placed at 23 km and 127 km from the feed end of the pipeline respectively, which were activated at 800 s following the failure at a rate of 2.56 cm s^{-1}. Furthermore, the simplifying assumption was made that prior to the release the CO_2 fluid was stagnant in the pipeline. In simulations the closed-end boundary conditions were applied at both ends of the pipeline. It should be noted that the due to the length of the pipeline and the closure time of the valves used, the interaction of the flow with boundary conditions was expected to be minimal. Two sets of outflow calculations were performed using the PR equation of state. The first case accounted for a realistic topography of the pipeline as shown in Figure 3, while in the second case a horizontal pipeline indicating a flat terrain was modelled. Figure 3 also shows a comparative plot of the depressurisation history, in terms of the pressure at the release point, for both the cases studied for the upstream section of the pipeline. As can be seen, the resulting outflow predictions are relatively insensitive to the differences in pipeline inclination. There are only minor differences in the release pressures predicted in the initial

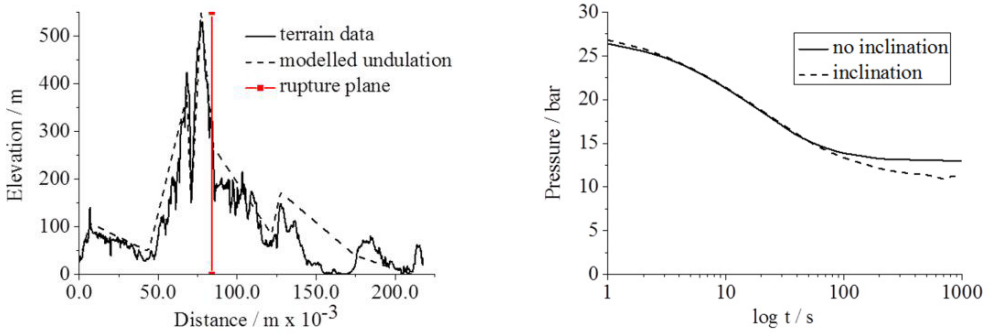

Fig. 3. Elevation variation along pipeline route (left) and predicted release pressure from upstream section of ruptured pipe (right), plotted against time for cases with and without inclination.

stages, although these differences become more significant towards the end of the simulation. This lack of impact is explained by the relatively small contribution of the hydrostatic head to the total pressure in the pipeline during the initial period of its depressurisation.

2.1.4. WP1.4 - Near-field dispersion model

Predictions were based on the solutions of the density-weighted averaged forms of the transport equations for mass, momentum, two conserved scalars (CO_2 mass fraction and CO_2 dense phase fraction), and total energy per unit volume (internal energy plus kinetic energy). This model is capable of representing a fluid flow-field comprising a mixture of CO_2 (vapour/liquid/solid) and air. The equations employed in this study were cast in an axisymmetric two-dimensional geometry for the purpose of validatory calculations of pipeline punctures and full-bore ruptures, and extended to three dimensions for the 'real-case' scenario release incorporating a crater geometry. The equation set was closed via the prescription of the turbulence stress tensor and the implementation of the $k-\varepsilon$ turbulence model [21] where the Reynolds stresses are modelled using a Boussinesq approximation and a turbulence eddy viscosity, represented as a function of the turbulence kinetic energy and its dissipation, which in turn leaves the requirement for the additional solution of their respective transport equations.

Although the standard k-ε model has been extensively used for the prediction of incompressible flows, its performance is well known to be poor in the prediction of their compressible counterparts. The model consistently over-predicts turbulence levels and hence mixing due to compressible flows displaying an enhancement of turbulence dissipation. A number of modifications to the k-ε model have been proposed by various authors, which include corrections to the constants in the turbulence energy dissipation rate equation [22, 23], and to the dissipation rate itself [24, 25]. Previous works by the present author [26, 27] have indicated that for flows typical of those being studied here, the model proposed by Sarkar et al. [24] provides the most reliable predictions. This model specifies the total dissipation as a function of a turbulent Mach number and was derived from the analysis of a direct numerical simulation of the exact equations for the transport of the Reynolds stresses in compressible flows. Observations made of shock-containing flows indicated that the important sink terms in the turbulence kinetic energy budget generated by the shocks were a compressible turbulence dissipation rate, and to a lesser degree, the pressure-dilatation term.

The adaptive mesh-refinement (AMR) strategy [28] employed an unstructured finite-volume grid algorithm which requires an order of magnitude less memory, and hence provides an order of magnitude faster computation times than a structured approach. Approximation of the diffusion and source terms was undertaken using central

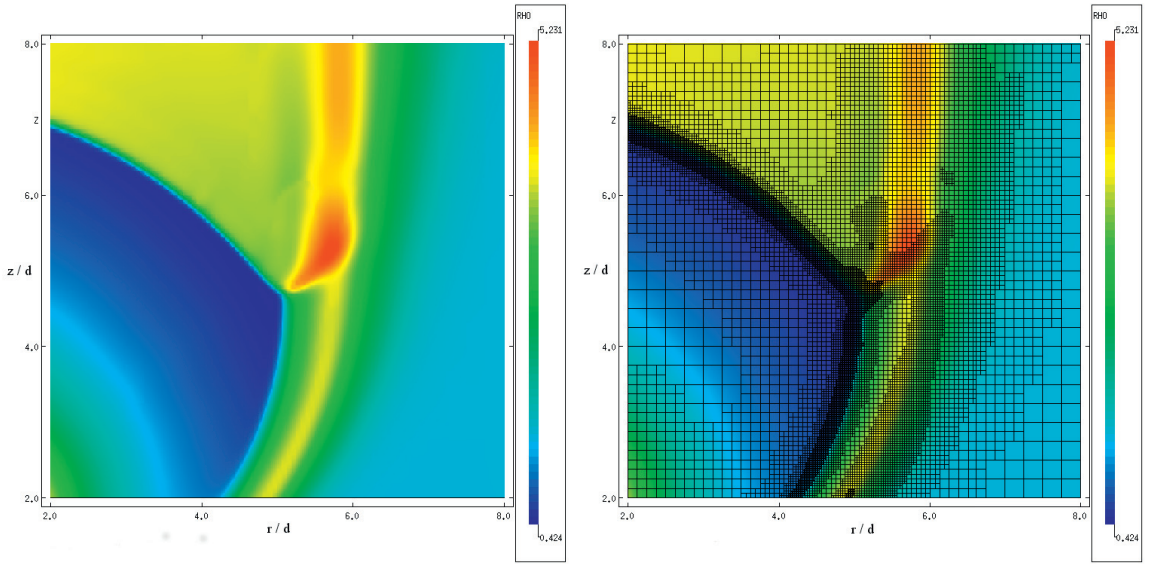

Fig. 4. Demonstration of AMR grid mapped over axial velocity predictions in a sample axisymmetric CO_2 jet calculation in the location of the sonic triple point.

differencing, and an HLL (Harten-Lax-Van Leer), second-order accurate variant of Godunov's method applied with respect to the convective and pressure fluxes. Figure 4 demonstrates the AMR technique as applied at the triple point of a predicted shock in a typical CO_2 jet release. Where there are steep gradients of variable magnitudes such as at flow boundaries or discontinuities such as the Mach disc, the mesh is more refined than in areas such as the free stream of the surrounding fluid. As noted, the model to describe the fluid flow-field was cast in an axisymmetric geometry for the validatory calculations of jet releases, with a full three-dimensional scheme applied to the crater calculations, although the use of symmetry boundaries aided a reduction in computational expense. A full description of the equations solved, and the algorithm employed is reported elsewhere [5, 29].

The high Joule-Thompson coefficient observed in high-pressure CO_2 expansions means that three phases may be present at any one time, and the thermophysics of such a complex and non-ideal system must be represented if accurate predictions are to be achieved. A composite equation of state has therefore been constructed. In this, the gas phase is computed from the Peng-Robinson equation of state [15], and the liquid phase and saturation pressure are calculated from tabulated data generated with the Span and Wagner [30] equation of state and the best available source of thermodynamic data for CO_2, the Design Institute for Physical Properties (DIPPRR) 801 database, access to which can be gained through the Knovel library [31]. Figure 5 shows the near-field temperature structure of a pure CO_2 jet release calculated in axisymmetry, and resulting from the application of three different equation of state approaches. The ideal equation of state predicts a width of the jet at the Mach shock 33% narrower than the Peng-Robinson equation of state, and 50% narrower than the composite equation of state. In the lower right panel of this figure we compare the temperatures along the jet axis. The ideal approach (dotted line) predicts 55 K just before the Mach shock, the Peng-Robinson (dashed line) 155 K and the composite (solid line) 168 K. Post-shock, when the pressure in the jet is close to atmospheric, solid and gaseous CO_2 coexist. In a homogeneous relaxation model, such as the one presented here, a mixture of pure two-phase CO_2 at atmospheric pressure must be on the saturation curve, at what is defined as the sublimation temperature: 194.675 K for CO_2 [32]. All three models predict 100% CO_2 at approximately atmospheric pressure in the core of the jet immediately after the Mach shock, allowing for an excellent test - the core of the jet should be at the sublimation temperature. The ideal equation of state predicts a

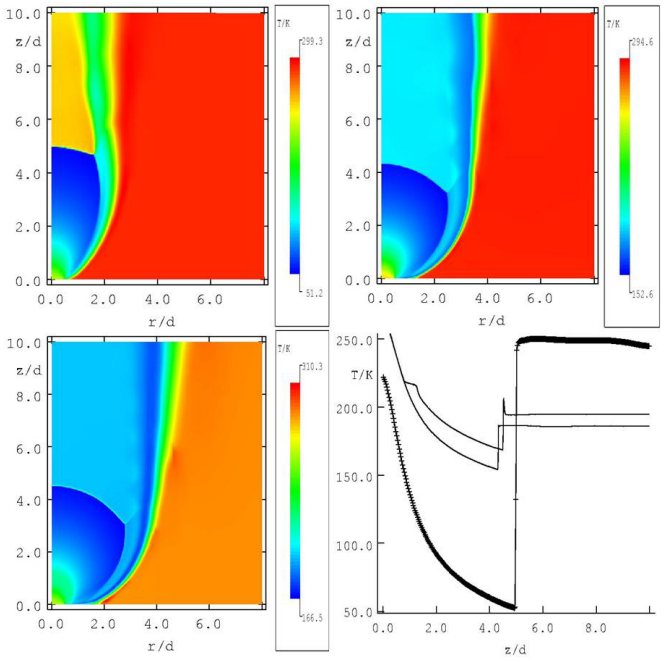

Fig. 5. Temperature predictions in the near-field using the ideal equation of state (upper left), the Peng-Robinson equation of state (upper right) and the composite equation of state (lower left), and axial profiles obtained using the ideal (markers), Peng-Robinson (lower solid curve) and composite (upper solid curve) models

Table 3. Pipeline parameters of the 'typical' crater release.

Pipeline Diameter / m	Pipeline Depth / m	Pipeline Temperature / K	Initial Pressure / Pa	Break Length / m	Exposed Pipe / m
0.914	1.0 (to top)	283.15	150×10^5	14.0	8.0

Table 4. Crater parameters of the 'typical' crater release.

Crater Length / m	Crater Width / m	Crater Depth / m	Crater Angle / degrees
30.0	12.0	4.0	45.0

high core temperature around 247.5 K, whereas the Peng-Robinson and composite equations of state predict 185.3 K and 193.9 K, respectively. The composite model is in excellent agreement with the sublimation temperature, the slight difference due to the fact that the pressure immediately after the Mach shock is approximately 5% lower than atmospheric. The low temperature predicted by the Peng-Robinson equation is a demonstration of how the model-predicted saturation pressure diverges from the real saturation pressure going below the triple point.

The purpose of the development of a full three-dimensional model incorporating realistic thermophysics is the study of cases representative of full-scale releases, including full-bore guillotine ruptures of high-pressure CO_2 transport pipelines. This work forms part of a demonstration of a 'whole-system' capability, incorporating outputs from a number of WPs. In-pipe modelling, and hence pipe-outflow data generated in WP1.3, are passed to this WP (WP1.4) as initial conditions for the near-field dispersion model, the output of which being passed to WP1.5 to perform the far-field CO_2 dispersion calculations. A crater geometry, typical of high-pressure pipeline rupture, has been chosen based upon observation of data and theory presented in the literature [33]. The general shape of the crater at ground level is elliptical, and further parameters detailing the pipeline conditions and crater shape are given in Tables 3 and 4 respectively. This geometry has been incorporated into a three-dimensional model, and Figure 6 shows an example of such a set-up. Figure 6(a) depicts a cut along the centreline on the y-axis, which lies along the centre of the release pipe at x=0. The z dimension represents the crater depth, and symmetry boundaries are located at x=0 and y=15 m. Figure 6(b) is looking down on to the crater top. The axisymmetric left boundary at x=0 can be seen to bisect the pipe. As previously mentioned, the uppermost boundary at y=15 m is also axisymmetric, and represents the companion jet release in a symmetrical full-bore scenario. Figure 7 shows sample predictions of a typical release obtained from the application of this crater geometry, with initial conditions (pressure, temperature, density, velocity and phase composition) provided by the pipe outflow model. Depicted are dense-phase CO_2 mass fraction, and total velocity predictions, and the features of such a highly under-expanded jet can be seen, including the formation of a Mach disc, and the acceleration of the flow to supersonic velocities.

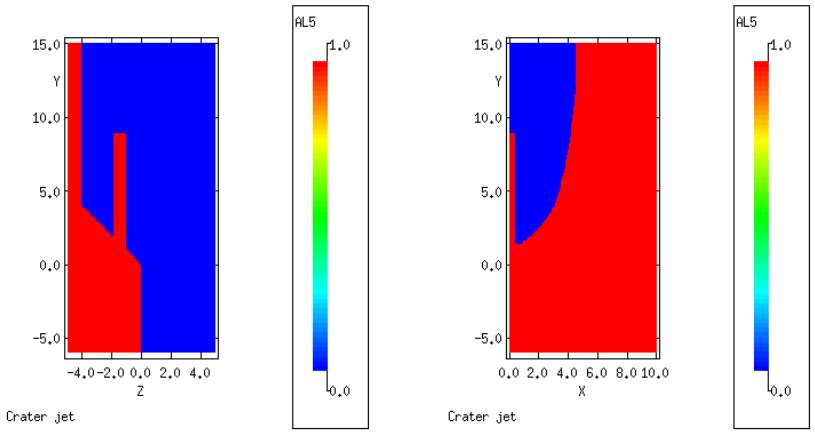

Fig. 6. Sample three-dimensional geometry of a typical full-bore guillotine rupture into an elliptic crater. (a) View at x=0 depicting the crater length, and (b) view at z=0 depicting the crater plan.

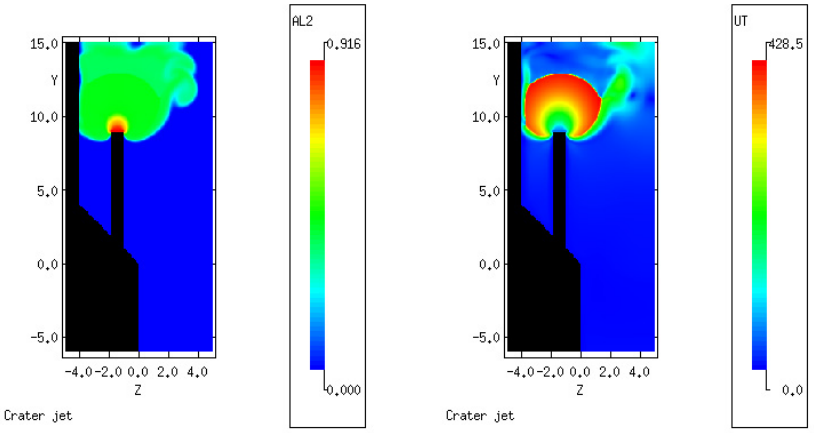

Fig. 7. Sample three-dimensional model predictions of a typical full-bore guillotine rupture into a crater. Dense-phase CO2 predictions (a) and total velocity (b).

Predictions derived from this model were then used as source terms for far-field dispersion calculations undertaken in WP1.5. Further details regarding the source modelling, and results obtained from these calculations can be found Section 2.0.5.

2.1.5. WP1.5 Far-field dispersion model

The chief objective of WP1.5 was the modelling of far-field dispersion of carbon dioxide resulting from accidental pipeline releases, including the importance of terrain and the wind-field on the dispersion behaviour. This was undertaken using two different commercial computational fluid dynamic codes: FLACS [10]; and ANSYS-CFX [11]. In both cases, the continuous gas-phase was solved in the Eulerian reference frame, whilst a Lagrangian formulation was used for the dispersed particle phase. When dealing with poly-dispersed turbulent two-phase flows, the Lagrangian reference frame appears to be the natural choice for treating the dispersed phase, in which individual particles or representative numerical particles, are tracked and their characteristics are evaluated as they move through the turbulent flow field. Moreover, this approach is well adapted for modelling particle interactions with obstacles and particle deposition [34], which are processes that need to be accounted for in the systems studied here. Considered in the modelling are non-compressible, non-reacting fluid-particle flows without collisions between particles. The physical phenomena of interest are the dispersion, vaporization, and deposition of particles and the coupling between the continuous phase and the dispersed phase. Further information regarding the equations employed and the solution methods applied can be found in [11] and [35]

Both far-field models employed the same source boundary conditions, where the CO_2 jet conditions at the inlet plane were taken from the near-field dispersion model outputs, as described in section 2.1.4, which consisted of integrated planar profiles of velocity, temperature, CO_2 solid and vapour concentration, turbulence kinetic energy and its dissipation rate. The size of the CO_2 particles produced by dense-phase CO_2 releases is uncertain, and it cannot be measured reliably in large-scale releases. However, previous work has shown that homogeneous equilibrium (HE) dispersion models provide reasonably good predictions of temperatures and concentrations in dense-phase CO_2 jets produced by orifices up to 50 mm in diameter [36, 37]. These HE models assume that the particles have the same temperature and velocity as the surrounding gas phase, which implies that the particles must be very small. Analysis of CO_2 particle sizes by Hulsbosch-Dam, et al. [38] has also suggested that their initial diameter once the jet has expanded to atmospheric pressure should be in the range 1 – 20 μm. In the current CFX simulations, the CO_2 particles are assigned an initial uniform diameter of 20 μm, whereas a log-normal or uniform diameter distribution is used in FLACS with different initial diameter sizes.

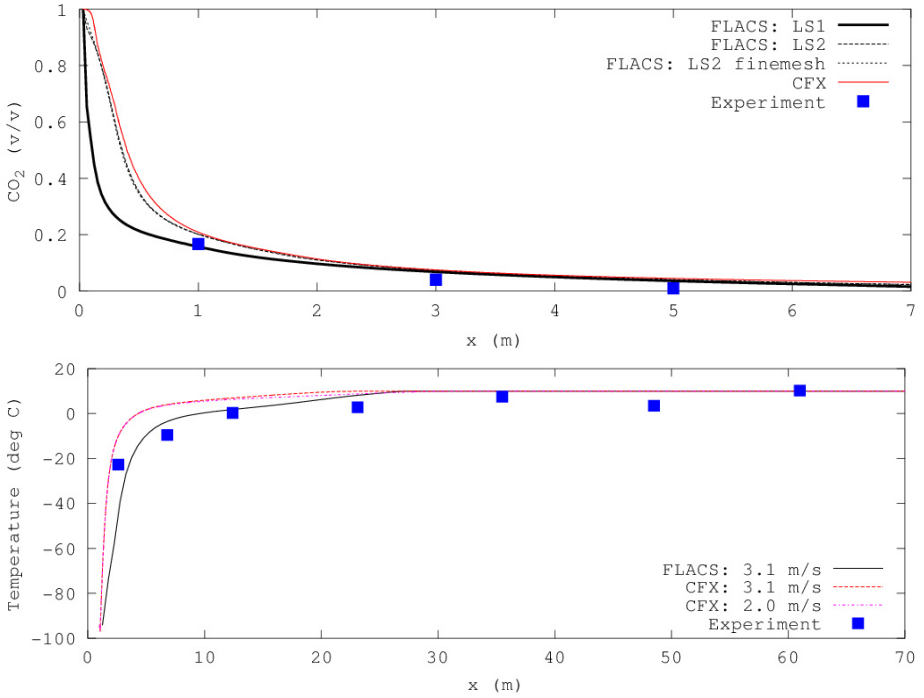

Fig. 8. Volume fraction of CO_2 predicted by FLACS and CFX models in the small-scale experiments of INERIS (Test 2 in WP2.1) (top), and temperature predictions of the industrial-scale experiments of DUT (WP2.1) (bottom).

Validation of the far-field models was first undertaken against data obtained from the experimental investigations reported in Section 2.1. Figure 8 depicts sample results obtained from application of both CFX and FLACS to both medium- and large-scale releases in terms of CO_2 volume fraction and temperature predictions, along their centreline. LS1 and LS2 in Figure 8 correspond to two different turbulent length-scales, both adopted as source in the FLACS simulations, and LS2 being used in the CFX simulation, and a good level of agreement can be seen between experimentation and predictions.

In order to demonstrate the model capabilities for a realistic accident scenario, the hypothetical pipeline release in 'realistic' terrain geometry was considered. The digital terrain data obtained from the Ordnance Survey was successfully imported into FLACS and CFX, and following wind build-up simulations in FLACS and CFX, the data resulting from the near-field predictions in WP1.4 was integrated as a source in the current far-field models. The length and width of the domain size in each case is 10 km and 5 km respectively. The FLACS domain extended to a height of approximately 1 km, whilst a lesser height was used in CFX, which varied from 260 m to 610 m depending upon the location. The computational grids used in the two codes were very different as FLACS employed a multi-block Cartesian mesh with 2.7 million grid points, whilst CFX used an unstructured grid of 3.2 million nodes that was composed of mainly tetrahedral cells, with prism-shaped cells along the solid boundaries. A steady-state solver was used for the CFX simulations, and the default transient flow solver was used in FLACS.

The predicted CO_2 jet in the vicinity of the crater is shown in Figure 9 for the FLACS and CFX models. Owing to the smaller particle-size used in the CFX simulations, it was found that all of the particles sublimated within the airborne jet. In contrast, the larger initial particle-size prescribed in the FLACS simulations resulted in some solid-CO_2 mass raining-out on to the terrain. Towards the end of the FLACS simulation, it was recorded that approximately 20% of the total mass discharged, at around 550 tonnes, had rained-out on the ground. This result suggests that banks of solid CO_2 might be formed in CO_2 pipeline releases if particles with diameters of the order 300 μm or larger are produced in the jet leaving the crater.

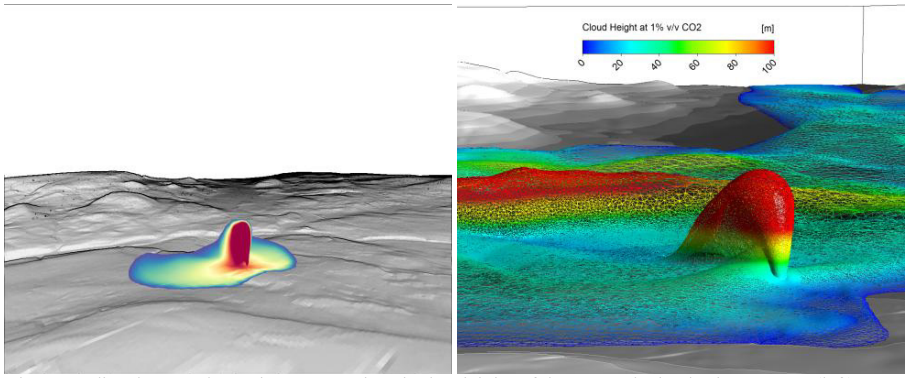

Fig. 9. Predicted CO_2 volumetric concentrations in the vicinity of the crater obtained using FLACS (left) and cloud height at 1 % concentration obtained using CFX (right).

Figure 10 shows the steady-state cloud predicted by the CFX code in terms of CO_2 concentration as a function of distance from the release source at 1 m above ground level. At low concentrations of 1% or 2%, CO_2 is considered not harmful but these concentrations may correlate to the extent of the visible cloud due to condensed water vapour (i.e. mist). A concentration of 4% v/v CO_2 corresponds to the immediately dangerous to life and health (IDLH) value recommended by [39]. The CFX results show that even with a wind speed of 5 m s^{-1}, the presence of the terrain has a large effect on the dispersion of the CO_2 cloud, and rather than being blown downwind, the cloud spreads mostly in the lateral directions, up and down the valley.

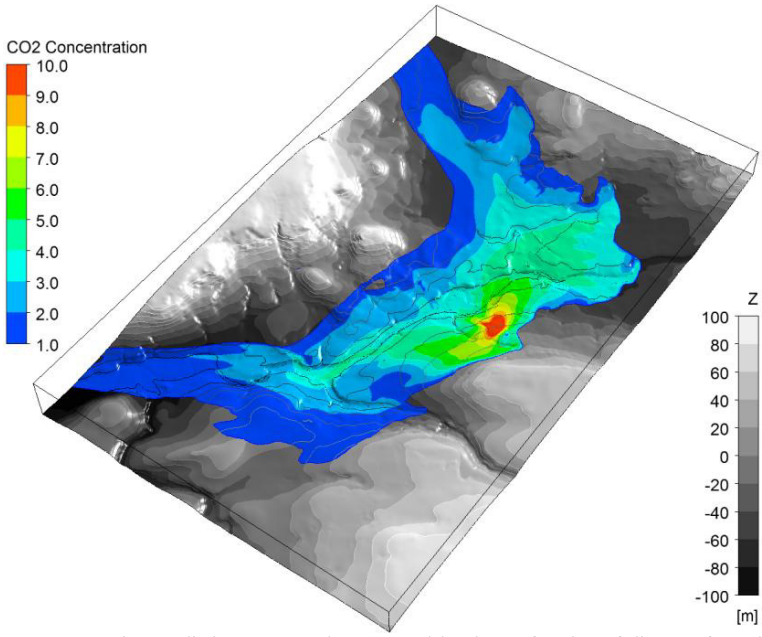

Fig. 10. CO_2 concentration predictions at 1 m above ground level as a function of distance from the release source in realistic terrain.

Figure 11 depicts results obtained from FLACS at the end of the simulation, which corresponds to a physical time of 538 s. Shown are predictions of CO_2 volume fraction, temperature, bulk mean velocity and density, above ground level.

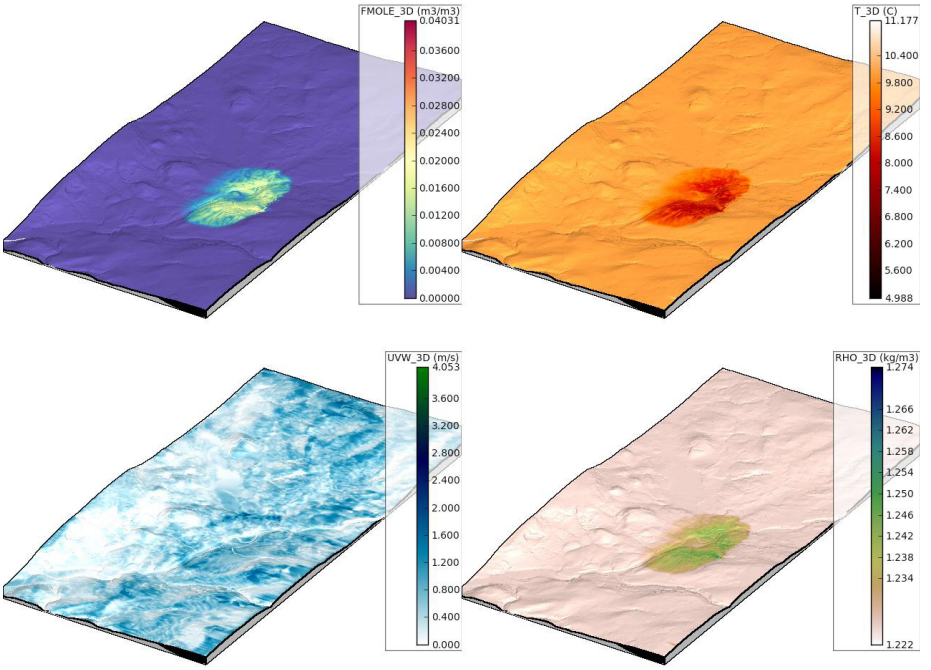

Fig. 11. Predictions of CO_2 volume fraction (v/v), temperature (°C), bulk mean velocity (m s^{-1}), and density (kg m^3), at ground level.

2.2. WP2 - Experimental data and validation

In this WP, experimental means were developed to investigate the thermophysical properties of CO_2-impurities mixtures, to study the fluid flow pattern inside the pipe during a release, and to analyse the flow rate and structure of the ensuing sonic jet in the near field. Significant effort was also devoted to the development of robust instrumentation to aid in the challenging task of industrial-scale experimental measurements undertaken in WP2.2 It was also possible to gain information for the dispersion behaviour of CO_2 in the far field.

2.2.1. WP2.1 - Small scale experimental investigation

To determine the thermophysical properties of CO_2-impurities mixtures, a small scale set-up was designed. It consists of a small (0.001 m^3) high pressure reservoir used as an adiabatic calorimeter (i.e. strongly insulated) provided with an opening and with a discharge duct. The pressure and temperature inside is carefully metered and the mass content is accurately controlled. The discharge duct can be thermally regulated and the heat losses and temperature variations can be measured. A heating cord is wrapping around the reservoir below the insulation and used whenever needed to control the initial conditions of the experiments. When the valve is open, the content of the calorimeter discharges very slowly (quasi-homogeneous and reversible conditions) so that from the energy and mass evolution, thermodynamic properties can be estimated while the pressure losses and temperature changes along the discharge line give access to the viscosity and thermal conductivity. In particular CO_2-air (0-3%v/v) and CO_2-O_2 (0-3%v/v) mixtures were investigated. Among the various measurements, the location of the vapor–liquid equilibrium (VLE) could be found and recorded. Further detail regarding the experimental set-up can be found in Proust, et al. [40].

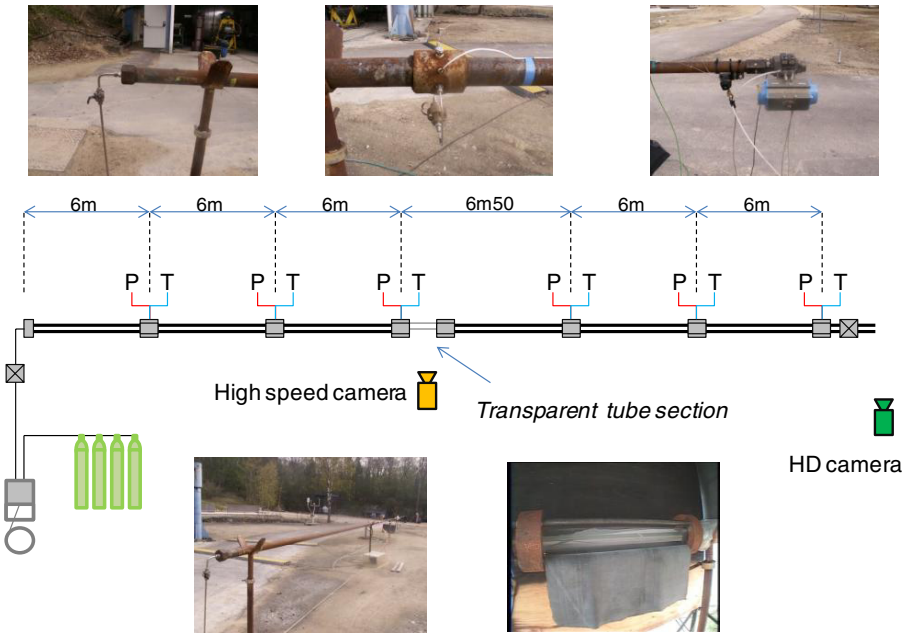

Fig. 12. Small scale setup to investigate the fluid flow pattern inside the pipe during experiments.

To study the fluid flow pattern inside the pipeline during a release, a 40 m long, 50 mm inner-diameter straight pipe was built. The fluid pressure and the temperature could be measured every 6 m and a transparent section was inserted half way along the pipe (Figure 12) to observe flow patterns. The orifice size could be varied from a small puncture (6 mm) to a full bore rupture. CO_2-N_2 (0-3%v/v) mixtures were used, with initial temperatures between 293 K and 308 K, and initial pressure of 100 bar. Among other results it was demonstrated that, except in case of a full bore rupture, the flow in the pipe is strongly stratified, with boiling liquid on the bottom and vapour on the top, and that the flow rate and thermodynamic characteristics of the line exterior flow depend very strongly on this stratification process.

The third experimental set-up aimed at analysing the characteristics of the near-field jet, mass flow rate, and downstream dispersion behaviour. A highly insulated 2 m^3, high-pressure vessel was used as a buffer reservoir with a maximum working pressure and temperature of 200 bar, and 473K respectively. This was coupled with a short 6 m release pipe located at the bottom of the vessel so that only liquid could flow out. The end of the pipe was equipped with an orifice to vary the release rate between 6 mm and full bore of 50 mm. Temperatures and pressures in the near field of the release were carefully measured in addition to the instantaneous mass flow rate by recording the weight of the vessel during a release. Further information regarding the experimental rig and measurement technique can be found in Jamois and Proust [8].

The undertaking of the above experimentation permitted both the preparation of the large scale experiments in WP2.2 and provided the consortium with a set of unique data covering most of the spectrum of the project, including: thermodynamic/transport properties of CO_2-impurities mixtures (WP1.2), flow patterns inside the pipeline during a release (WP1.3), mass flow rates and near field jet (global) structure in relationship with the fluid flow pattern (WP1.4) and dispersion of CO_2 in the far field (WP1.5).

2.2.2. WP2.2 - Industrial scale experimental investigation

The design and construction of the large scale experimental set-up in WP2.2 was the most technically challenging aspect of the CO2PipeHaz project. Despite the delay in the start of the large scale experiments due to the unprecedented weather conditions in China in summer 2011, the work package progressed in accordance with the

Fig. 13. High speed CO_2 jet following full bore rupture release test from an initial pressure and temperature of 36 bar and 3 °C.

project description of work, meeting its objectives and deliverables. Figure 13 shows the high speed jet during the full bore rupture test, 2 s after the initiation of the release.

The world's first industrial scale CO_2 pipeline (256 m long, 233 mm i.d. and 20 mm wall thickness) for performing CO_2 release experiments was constructed and fully instrumented. The set-up was used to perform tests for the validation of theoretical models of CO_2 outflow and dispersion. The detailed design and construction of the experimental facilities are described elsewhere [41]. The test pipeline was equipped with a data acquisition system for the synchronous recording of temperature and pressure signals at various locations on the pipe, and the release tests were initiated using a specially-designed dual bursting-disk device.

Four CO_2 fully-instrumented release experiments were performed including three orifice releases (50 mm orifice) and one full bore rupture release (FBR). A large amount of data was recorded and analysed both within the pipeline and in the dispersion area, and Figure 14 depicts CO_2 concentration calculated from collected temperature data in the near-field dispersion region of a 36 bar release.

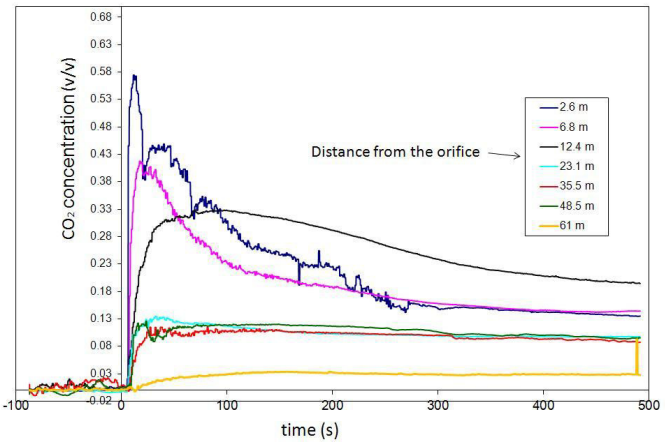

Fig. 14. Calculated CO_2 concentrations at different positions in the dispersion area along the centre-line axis of the jet.

2.3. WP3 - Decision support tools

Lead by the Health and Safety Laboratory in the UK, WP3 was focussed at reviewing design good practice for CO_2 pipelines and at developing a risk assessment methodology. Objectives included the embodiment of the understanding and predictive capabilities developed into decision support tools, the assessment and improvement of existing safety through the development of risk assessment methods and tools for CO_2 pipeline application, and to produce refined best-practice guidelines. Ultimately a test-case was planned to demonstrate the developed tools' usefulness.

Initially, a review of dense gas dispersion models was undertaken that are able to account for the effects of topography. Two types of dispersion models were identified as having the potential to be used in CO_2 pipeline quantitative risk analysis (QRA) studies, these being shallow layer and Lagrangian particle-tracking models. The shallow-layer model, TWODEE-2, was used to generate 1 %, 10 % and 50 % fatality-risk contours for a series of release points along a hypothetical, but representative, 1 km-long section of a CO_2 pipeline. Individual and societal risk values were calculated and represented geographically using HSL's quantitative risk assessment tool QuickRisk and dose contours extracted from TWODEE-2 outputs. The calculated risk values were compared to those generated from an integral dispersion model. This comparison highlighted the effect that topography can have on dispersion results and on the calculated individual and societal risk levels in the vicinity of CO_2 pipelines. It was recommended that, ideally, risk assessment of high-pressure CO_2 pipelines use consequence assessment tools that are able to account for the effect of topography in an appropriate manner. The use of integral models that ignore terrain may not ensure that adequately realistic or conservative harm contours are used to calculate risk in areas of complex topography. However, until suitable models become available that can take into account the effects of topography, 'flat-earth' integral models should continue to be used. CFD models are generally too slow to run to be used for QRA purposes, but it may be necessary to use them in certain limited circumstances when the topography has a significant effect on the risk assessment or to investigate the impact of specific terrain features. Further work is

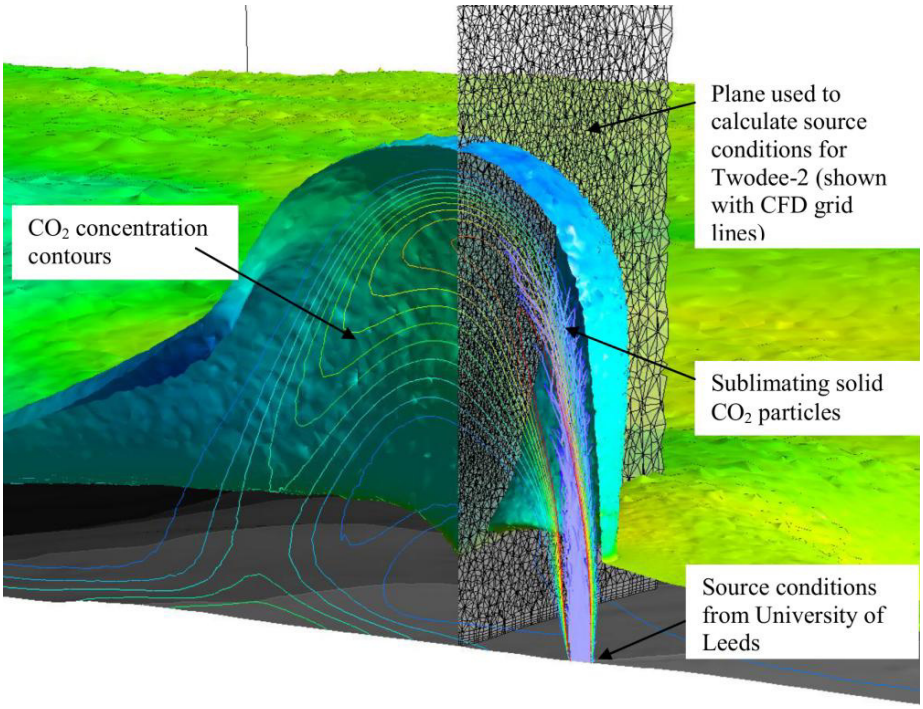

Fig. 15. Cross-section through the jet in the ANSYS-CFX model, showing the vertical plane used to calculate the source conditions for the TWODEE-2 model.

needed to develop and validate shallow-layer dense gas dispersion codes suitable for application to high-pressure CO_2 pipelines.

While TWODEE-2 appears to be well-suited for this particular application, issues with the model have been previously identified that mean that the model could not be recommended for use in practice. To illustrate this point, it was shown that TWODEE-2 model predictions show significant differences compared to those generated from a fully three-dimensional CFD dispersion model. On-going work at HSL is seeking to develop an alternative to TWODEE-2. In the meantime, it is used here solely to demonstrate the principle of embedding a shallow-layer model into a QRA. Currently, the way in which the source of CO_2 is represented in dispersion models is uncertain, due to the complex thermodynamic properties of CO_2, the potential for releases to form solid CO_2 particles, and the complex flow behaviour within pipeline craters. Figure 15 depicts a cross-section through a predicted release obtained using the ANSYS-CFX model, showing the vertical plane used to calculate the source conditions for the TWODEE-2 model. There are however key knowledge gaps that need to be addressed. It should be acknowledged that dispersion model predictions, particularly when including topography, may be sensitive to the way in which the CO_2 source is represented.

Subsequent to the review of existing dense-phase gas dispersion models, and the identification of knowledge gaps, a risk assessment methodology based on the ARAMIS methodology for assessing CO_2 pipelines safety was undertaken. The accidental risk assessment methodology for industries (ARAMIS) was developed within the fifth framework program of the European Commission, and aims at proposing a risk assessment methodology that takes into account major accidents prevention measures in risk assessment of an industrial plant. The methodology of ARAMIS was analysed step by step considering CO_2 pipelines issues and then, knowledge gaps were filled in order to propose a failure frequency coherent with CO_2 pipelines accidental data and breach sizes also in accordance with CO_2 pipeline accident data. The use of the feedback available for CO_2 pipelines was connected with the data available for natural gas and hydrocarbons pipelines. The goal of this was first, to propose a methodology for assessing CO_2 pipelines which results from the ARAMIS concepts but which is adapted to the specificity of CO_2 transport and then, to propose data to be used in the quantitative element of the methodology. Those data were then used for probability estimation, while consequences modelling developed in other WPs of the project was used for intensity and gravity estimation. Only land-transmission pipelines are of concern in the scope of this study, and offshore pipelines are not studied. The consideration of sub-sea pipeline transmission is one which has not been considered to date, and can be identified as a knowledge gap urgently requiring addressing.

Given the above findings, good practice guidelines were drafted [42] which cover decision support tools including risk assessment for CO_2 pipelines. These guidelines provide a road map identifying the most relevant sources of guidelines including general guidelines for hazardous pipelines, existing guidelines for CO_2 installations and pipelines, and new knowledge produced by CO2PipeHaz. Additionally, a test case-study was undertaken which provides an example of the use of the methodologies developed in WP3 for a test-case pipeline. Specifically, a QRA incorporating integral modelling has been carried out and used to target the consideration of potential additional risk reduction measures for a hypothetical pipeline. It was demonstrated that results can be used as an input to decision support, by identifying the locations of the high risk segments of the pipeline. It was concluded by Wardman and Wilday [43] that the CO2PipeHaz Good Practice Guidelines [42] should be used to identify and consider further risk reduction for those parts of the pipeline identified as being of sufficiently high risk.

3. Conclusions

The development of methods and equations of state capable of predicting the phase equilibria, thermodynamic and transport properties of CO_2 and CO_2 mixtures over the wide range of fluid conditions likely to be encountered was undertaken WP1.2. A model for predicting the multi-phase heterogeneous flow of CO_2 and CO_2 mixtures within and on leakage from pipelines using the models developed in WP1.2 was presented in WP1.3. This allows the prediction of discharge rates and the fluid state during pipeline failure and depressurisation, and the investigation of methods for mitigating against such losses.

The results of both small and large-scale experiments indicated the limitations of the homogeneous equilibrium model in simulating outflow following dense phase CO_2 pipeline rupture. This is primarily due to the presence of phase-slip and delayed liquid/vapour phase transition during the rapid depressurisation process, both of which are

not accounted for in the HEM. In the case of punctures, visual observation of the in-pipe flow profiles by INERIS has indicated the prevalence of both phenomena. However, in the case of full bore rupture, only delayed phase transition has been found to be prevalent. As part of WP2, a homogeneous relaxation model accounting for delayed phase transition was developed, and in the case of pure CO_2 the HRM was found to produce improved predictions of the pipeline decompression and discharge rates as compared to the HEM.

Mathematical models capable of predicting the near-field structure of high pressure releases of supercritical and multi-phase carbon dioxide, including models for the formation of liquid droplets and solid particles, subsequently required in order to provide input into far-field dispersion models, and to allow assessments of the near-field impact of CO_2 releases, was undertaken in WP1.4. The complete model, developed using both established and novel techniques, yielded excellent predictions of the characteristics of sonic CO_2 jets, in comparisons with experimental data generated in WP2.1. Additionally, the complete model was successfully applied to the prediction of the industrial scale investigations undertaken by DUT in WP2.2, and to the 'realistic terrain' demonstration case. This case shows that it is feasible to use complex three-dimensional CFD models to predict the dispersion of CO_2 over complex terrain. In practice, CFD models are unlikely to be used on a routine basis for risk assessment of CO_2 pipelines, since the computer run times are of the order of days to weeks for just a single simulation. Instead, integral or shallow-layer models are more likely to be used for routine calculations. However, this demonstration case has shown that if a particularly complex scenario needs to be investigated, such as one where there are large obstacles or significant terrain effects, then it is possible to examine these effects using CFD models.

In addition to the theoretical developments noted above, the unique small and large scale experimental facilities developed for the validation and the provision of the relevant thermophysical data offer significant scope for conducting further research on hazard assessment of CO_2 pipelines enveloping a more diverse range of stream impurities and wider ranges of operating temperatures and pressures than those considered during the course of the CO2PipeHaz project. These facilities which are fully available for research exploitation included a novel calorimetric technique constructed by INERIS for measuring CO_2 transport properties and its mixtures. This consisted of a 1 litre flow calorimeter linked to a calibrated and thermally regulated discharge line, which allows the simultaneous measurements of the enthalpy, specific heat, density, viscosity and thermal conductivity of pure CO_2 and CO_2/impurities mixtures in a single flow experiment. A limited amount of data has been obtained to date, but the potential of the technique has been established. A number of scientific questions were answered, including the position of the vapour-liquid equilibrium lines and the dissolution process of CO_2/impurities mixtures as the pressure is reduced. Densities have been measured of the condensed phase revealing a decrease of the density of CO_2 while the amount of impurities increases. On the basis of presently available experimental evidence, no discernible impact of the impurities on the CO_2 transport properties was observed.

The fully instrumented 40 m pipe constructed by INERIS as part of WP2.1 for the first time allowed the direct observation of the in-pipe flow patterns during pipeline rupture, including the detailed study of the near-field jet structures. Additionally, the fully instrumented, temperature controlled, 250 m long pipeline constructed in China by DUT is the longest CO_2 test pipeline of its kind anywhere. This facility has allowed realistic pipeline rupture experiments, minimising the uncertainties associated with scale-up of the data. The results of the above experiments revealed some interesting features of CO_2 releases. In particular, the discharge of solid CO_2 particles formed in the pipeline during its decompression was observed in the full-bore rupture release experiment. In the puncture release tests the pressure measurements in the flow at various locations along the pipe length showed temporary stabilization of pressure near the triple point (5.18 bar) during the latter stages of decompression. This phenomenon was predicted by the outflow model developed in WP1.3, and is attributed to the liquid-vapour to solid-vapour phase transition at the triple point of CO_2, where the temperature reaches –56.8 °C.

The understanding and predictive methods developed through the research components of the project, described above, were embodied within decision support tools in WP3. Under this work package, existing good practice guidelines were identified and consolidated, together with the findings of this project, to produce refined good practice guidelines. Relevant and existing risk assessment methods and tools were reviewed, and a gap analysis undertaken. An integrated consequence assessment methodology was developed, with new knowledge generated from WP1 and WP2 used to fill the gaps in current methodologies, and to permit the development of a risk assessment methodology using integral consequence-modelling. Additionally, short-cut risk assessment

methodologies were considered and adapted, or developed as required. Overall, this work package delivered a range of decision support tools for use in the safe design and operation of CCS systems.

Lastly, and in order to promote uptake of the knowledge and technologies developed within the project, demonstration of their usefulness was carried out by their application to a test case in WP3 [43]. By this means, the usefulness of all the work performed, to the safe and commercial deployment of power generation technology based on CCS has been demonstrated.

Acknowledgements

The research leading to the results described in this paper has received funding from the European Union 7th Framework Programme FP7-ENERGY-2009-1 under grant agreement number 241346. The paper reflects only the authors' views and the European Union is not liable for any use that may be made of the information contained herein.

The contribution made to this paper by Simon Gant, was also part-funded by the Health and Safety Executive, UK. The contents, including any opinions and/or conclusions expressed, are those of the authors alone and do not necessarily reflect HSE policy.

References

[1] CO2PipeHaz. Quantitative Failure Consequence Hazard Assessment for Next Generation CO_2 Pipelines: The Missing Link, 2009. Accessed 01/07/14; [CO2PipeHaz Project Website]. Available from: http://www.co2pipehaz.eu/.

[2] Cowley LT, Tam VHY. Consequences of Pressurised LPG Releases: The Isle of Grain Full Scale Experiments. in GASTECH 88 - 13th International LNG/LPG Conference. 1988. Kuala Lumpur.

[3] Richardson SM, Saville G, Isle of Grain Pipeline Depressurisation Tests - OTH 94 441, 1996: HSE Books.

[4] Brown S, Martynov S, Mahgerefteh H, Proust C. A Homogeneous Equilibrium Relaxation Flow Model for the Full Bore Rupture of Dense Phase CO_2 Pipelines. Int. J. Greenh. Gas Con. 2013; 17: 349-356.

[5] Woolley RM, Fairweather M, Wareing CJ, Falle SAEG, Proust C, Hebrard J, Jamois D. Experimental Measurement and Reynolds-Averaged Navier-Stokes Modelling of the Near-Field Structure of Multi-phase CO_2 Jet Releases. Int. J. Greenh. Gas Con. 2013; 18: 139-149.

[6] Wareing CJ, Fairweather M, Falle SAEG, Woolley RM. Validation of a Model of Gas and Dense Phase CO_2 Jet Releases for Carbon Capture and Storage Application. Int. J. Greenh. Gas Con. 2013; 20: 254-271.

[7] Diamantonis NI, Economou IG. Evaluation of Statistical Associating Fluid Theory (SAFT) and Perturbed Chain-SAFT Equations of State for the Calculation of Thermodynamic Derivative Properties of Fluids Related to Carbon Capture and Sequestration. Energ. Fuel. 2011; 25: 3334-3343.

[8] Jamois D, Proust C, Hebrard J, Gentilhomme O. La Sécurité du Captage et du Stockage du CO_2: Un Défi pour les Industries de L'énergie Récents Progrès en Génie des Procédés 2013; 104.

[9] Wareing CJ, Woolley RM, Fairweather M, Falle SAEG. A Composite Equation of State for the Modelling of Sonic Carbon Dioxide Jets. AIChE J. 2013; 59: 3928-3942.

[10] GexCon AS. FLACS v10.0 User's Manual, 2013. Accessed 12/08/13; Available from: http://www.flacs.com.

[11] ANSYS. ANSYS CFX-Solver Theory Guide - Release 14.0. ANSYS Inc. 2011.

[12] Porter RTJ, Fairweather M, Pourkashanian M, Woolley RM. The Range and Level of Impurities in CO_2 Streams from Different Carbon Capture Sources. Int. J. Greenh. Gas Con. 2014; (submitted).

[13] Chen S, Zhang Y. CO2PipeHaz Internal Report: CO_2 Purification Requirements, the Associated Technology and Cost Estimate. Deliverable 1.1.2, Dalian University of Technology. 2011.

[14] Collard A, Chen S, Zhang Y. CO2PipeHaz internal report: Determination of the Optimum Composition Range for CO_2 Streams During Pipeline Transport. Deliverable 1.1.3, University College London and Dalian University of Technology. 2011.

[15] Peng D-Y, Robinson DB. A New Two-Constant Equation of State. Ind. Eng. Chem. Fun. 1976; 15: 59-64.

[16] Kunz O, Klimeck R, Wagner W, Jaeschke M. The GERG-2004 Wide-range Equation of State for Natural Gases and Other Mixtures. GERG Technical Monograph 15, GERG. 2007.

[17] Yokozeki A. Analytical Equation of State for Solid-Liquid-Vapor Phases. Int. J. Thermophys. 2003; 24: 589-620.

[18] Diamantonis NI, Economou IG. Modeling the Phase Equilibria of a H_2O-CO_2 Mixture with PC-SAFT and tPC-PSAFT Equations of State. Mol. Phys. 2012; 110: 1205-1212.

[19] Diamantonis NI, Boulougouris GC, Mansoor E, Tsangaris DM, Economou IG. Evaluation of Cubic, SAFT, and PC-SAFT Equations of State for the Vapor-liquid Equilibrium Modeling of CO_2 Mixtures with other Gases. Ind. Eng. Chem. Res. 2013; 52: 3933-3942.

[20] Woolley RM, Fairweather M, Wareing CJ, Proust C, Hebrard J, Jamois D, Narasimhamurthy VD, Storvik IE, Skjold T, Falle SAEG, Brown S, Mahgerefteh H, Martynov S, Gant SE, Tsangaris DM, Economou IG, Boulougouris GC, Diamantonis NI. An Integrated, Multi-scale Modelling Approach for the Simulation of Multiphase Dispersion from Accidental CO_2 Pipeline Releases in Realistic Terrain. Int. J. Greenh. Gas Con. 2014; 27: 221-238.

[21] Jones WP, Launder BE. The Prediction of Laminarization with a Two-Equation Model of Turbulence. Int. J. Heat Mass Tran. 1972; 15: 301-314.

[22] Baz AME. Modelling Compressibility Effects on Free Turbulent Shear Flows. in 5th Biennial Colloquium on Computational Fluid Dynamics. 1992. UMIST.
[23] Chen YS, Kim SW. Computation of Turbulent Flows Using an Extended k-ε Turbulence Closure Model. Document Number CR-179204, NASA. 1987.
[24] Sarkar S, Erlebacher G, Hussaini MY, Kreiss HO. The Analysis and Modelling of Dilatational Terms in Compressible Turbulence. J. Fluid Mech. 1991; 227: 473-493.
[25] Zeman O. Dilational Dissipation: The Concept and Application in Modeling Compressible Mixing Layers. Phys. Fluids A-Fluid 1990; 2: 178-188.
[26] Fairweather M, Ranson KR, Modelling of Underexpanded Jets Using Compressibility-Corrected, k-ε Turbulence Models, in *Turbulence, Heat and Mass Transfer 4*, K. Hanjalic, Y. Nagano, and M. Tummers, Editors. 2003, Begell House, Inc. p. 649-656.
[27] Fairweather M, Ranson KR. Prediction of Underexpanded Jets Using Compressibility-Corrected, Two-Equation Turbulence Models. Prog. Comput. Fluid Dy. 2006; 6: 122-128.
[28] Falle SAEG, AMR Applied to Non-linear Elastodynamics, in Proceedings of the Chicago Workshop on Adaptive Mesh Refinement Methods, T. Plewa, T. Linde, and V.G. Weirs, Editors. 2005, Springer Lecture Notes in Computational Science and Engineering v.41. p. 235-253.
[29] Falle SAEG. Self-Similar Jets. Mon. Not. R. Astron. Soc. 1991; 250: 581-596.
[30] Span R, Wagner W. A New Equation of State for Carbon Dioxide Covering the Fluid Region from the Triple-Point Temperature to 1100 K at Pressures up to 800 MPa. J. Phys. Chem. Ref. Data 1996; 25: 1509-1596.
[31] Imperial College London. DIPPR 801 Database, [Web database] 2013. Accessed 09/06/14; Available from: http://www.aiche.org/dippr/.
[32] Barber CR. The Sublimation Temperature of Carbon Dioxide. Brit. J. Appl. Phys. 1966; 17: 391-397.
[33] Kinsman P, Lewis J, Report on a Second Study of Pipeline Accidents Using the Health and Safety Executive's Risk Assessment Programs MISHAP and PIPERS, 2002: HSE Books.
[34] Crowe CT, Multiphase Flow Handbook. Mechanical and Aerospace Engineering Series, 2005, Bosa Roca, USA: CRC Press Inc.
[35] Narasimhamurthy VD, Pesch L, Skjold T. CO2PipeHaz Internal Report: FLACS Model Developments Including the Source, Wind and Terrain Models. Deliverable 1.5.3, GEXCON AS, Bergen, Norway. 2013.
[36] Dixon CM, Gant SE, Obiorah C, Bilio M. Validation of Dispersion Models for High Pressure Carbon Dioxide Releases. in IChemE Hazards XXIII. 2012. Southport, UK: IChemE.
[37] Witlox HWM, Harper M, Oke A. Phast Validation of Discharge and Atmospheric Dispersion for Carbon Dioxide Releases. in Proceedings of the 15th Annual Symposium, Mary Kay O'Connor Process Safety Centre. 2012. Texas A&M University, College Station, Texas, USA.
[38] Hulsbosch-Dam CEC, Spruijt MPN, Necci A, Cozzani V. Assessment of Particle Size Distribution in CO_2 Accidental Releases. J. Loss Prevent. Proc. 2012; 25: 254-262.
[39] National Institute for Occupational Safety and Health. Documentation for Immediately Dangerous to Life or Health Concentrations (IDLHs) for Carbon Dioxide, 1996. Accessed; Available from: http://www.cdc.gov/niosh/idlh/124389.html.
[40] Proust C, Jamois D, Hebrard J. CO2PipeHaz Internal Report: Experimental Investigation of the Thermodynamics of CO_2-impurities Mixtures. Deliverable 2.1.3, INERIS, France. 2013.
[41] Chen S, Zhang Y. CO2PipeHaz Internal Report: Report on Completed Discharge Measurement Through Different Diameter Orifices and Far-field Dispersion Investigations Including Data Analysis. Deliverable 2.2.3, DUT, China. 2012.
[42] Wilday AJ, Saw JL. CO2PipeHaz Internal Report: CO_2 Pipelines Good Practice Guidelines. Deliverable 3.5, HSL, UK. 2013.
[43] Wardman MJ, Wilday AJ. CO2PipeHaz Internal Report: Test Case for Decision Support. Deliverable 3.6, HSL, UK. 2013.